IEEE Access
Multidisciplinary | Rapid Review | Open Access Journal

Received 20 October 2023, accepted 5 November 2023, date of publication 9 November 2023,
date of current version 20 November 2023.

Digital Object Identifier 10.1109/ACCESS.2023.3331761

RESEARCH ARTICLE

Assessment of Spatiotemporal Variations in Wind Field Measurements by the Chinese FengYun-3E Wind Radar Scatterometer

YUE HE[1], HE FANG[1], XIAOHUI LI[2], GAOFENG FAN[1], ZHONGHUA HE[1], AND JUZHEN CAI[1]
[1]Zhejiang Climate Centre, Hangzhou 310017, China
[2]State Key Laboratory of Satellite Ocean Environment Dynamics, Second Institute of Oceanography, Ministry of Natural Resources, Hangzhou 310012, China

Corresponding author: Xiaohui Li (lixiaohui@sio.org.cn)

This work was supported in part by the National Natural Science Foundation of China under Grant 42306200 and Grant 42305153; in part by the Climate Change Special Project of the China Meteorological Administration under Grant CCSF202036; in part by the Natural Science Foundation of Zhejiang Province under Grant LQ21D060001; in part by the Fengyun Application Pioneering Project under Grant FY-APP-2021.0105; in part by the Science and Technology Project of Zhejiang Meteorological Bureau under Grant 2022ZD10 and Grant 2022ZD06; in part by the Scientific Research Fund of the Second Institute of Oceanography, Ministry of Natural Resources (MNR), under Grant JB2205; in part by the China Postdoctoral Science Foundation under Grant 2022M723705; in part by the Preferential Support for Postdoctoral Research Projects in Zhejiang Province under Grant ZJ2022041; in part by the Open Fund of the State Key Laboratory of Satellite Ocean Environment Dynamics, Second Institute of Oceanography, MNR, under Grant QNHX2222; in part by the Youth Innovation Team of the "Fengyun Satellite Remote Sensing Product Verification" of the China Meteorological Administration under Grant CMA2023QN12; and in part by the Satellite Special Project of China Meteorological Administration under Grant FY-3(03)-AS-12.13.

ABSTRACT The purpose of this study is to analyze the spatiotemporal variations in wind field measurements obtained from the Chinese FengYun-3E (FY-3E) Wind Radar (WindRAD) scatterometer. To assess the performance of the wind field retrievals, we compare the FY-3E WindRAD measurements to ERA5 winds, which is the fifth-generation reanalysis global atmosphere dataset from the European Centre for Medium-Range Weather Forecasts (ECMWF). The comparative analysis between FY-3E and ERA5 for the period from June 1, 2022, to December 31, 2022, reveals that FY-3E wind speed retrievals have a bias of −0.42 m/s and a standard deviation (STD) of 1.45 m/s. In comparison to the TAO/TRITON array observations, the wind speed retrievals show a bias of −0.70 m/s and a STD of 1.37 m/s. Further improvements in wind direction retrieval precision are necessary for the FY-3E WindRAD scatterometer to meet operational requirements, aiming for an error within 20Â°. Temporal variations in the bias and STD of FY-3E wind speed retrievals exhibit two states, primarily attributed to the improved precision in wind field accuracy resulting from the implementation of the ocean calibration bias correction and advanced inversion algorithms. The spatial distribution analysis reveals regions characterized by relatively high bias and STD values, which could be associated with the presence of sea ice contamination near the ice shelves in these areas. These findings have the potential to offer valuable insights for improving Earth's climate monitoring capabilities and enhancing the applications of oceanographic satellite observation systems.

INDEX TERMS FengYun-3E (FY-3E), wind radar (WindRAD), scatterometer, ocean surface wind field, wind assessment.

I. INTRODUCTION

Spaceborne microwave scatterometers play a pivotal role as a fundamental data source for acquiring global ocean surface wind field measurements in numerical weather prediction [1], [2]. Over the past 20 years, since the launch of the Active Microwave Instrument (AMI) on the European Remote Sensing (ERS)-1 satellite, several spaceborne scatterometers, including Seawinds and the Advanced Scatterometer (ASCAT), have provided continuous ocean wind data [3],

The associate editor coordinating the review of this manuscript and approving it for publication was Jethro Browell.

[4], [5], [6]. China has also contributed significantly to the field with its HaiYang-2 (HY-2) series of oceanographic satellites, which provide accurate ocean surface wind field (OSWF) data for global oceans. The CFOSAT (China-France Oceanography SATellite) is a collaborative deep ocean remote sensing satellite jointly developed by the China National Space Administration (CNSA) and the French National Centre for Space Studies (CNES) [7], [8], which offers high-resolution measurements of wind and waves simultaneously [9], [10], [11], [12], [13], [14], [15]. Assimilation of these data has enhanced the accuracy of weather forecasting and provided valuable insights into the Earth's climate system [16], [17], [18].

Compared with current spaceborne scatterometers, the Fengyun-3E (FY-3E) satellite's dawn–dusk polar orbit enables global coverage and fills the observational gaps of current numerical weather prediction models, making it effective in monitoring and analyzing various phenomena such as fog, forest fires, typhoons, and severe convection [19]. Additionally, its observations provide daily measurements in both infrared and microwave bands, significantly improving climate monitoring capabilities [19], [20]. In particular, the FY-3E satellite is equipped with the Wind Radar (WindRAD) system, which employs dual-frequency (C-band at 5.40 GHz and Ku-band at 13.256 GHz) and dual-polarization (horizontal HH and vertical VV polarization) scanning techniques to retrieve sea surface wind vectors, encompassing both wind speed and direction. Table 1 presents detailed information about the FY-3E orbit and the WindRAD sensor. FY-3E WindRAD has several advantages. First, the improved spatial resolution of the scatterometer enables the retrieval of global ocean surface wind fields closer to the coast, thus improving the forecasting of wave and wind hazards in coastal regions [21]. Second, WindRAD, with its unique configuration as a rotating fan-beam scatterometer and dual-frequency observations, has the potential to provide accurate measurements of high wind speeds. The unique capabilities of FY-3E, with improved spatial resolution and enhanced wind retrieval capability, are highly valuable for applications like severe weather monitoring, wind energy resource assessment, coastal weather hazard forecasting, tropical cyclone monitoring.

TABLE 1. Details of the Fengyun-3E (FY-3E) satellite orbit and the Wind Radar (WindRAD) scatterometer.

Parameters	Description
Orbit height	836 km
Inclination	98.75°
Local time at descending node	05:30–05:50 UTC
Quasi-repeat time	5.5 d (design 4–10 d)
Eccentricity	$\leqslant 0.0025$
Orbital maintenance	20 min (8 yr)$^{-1}$
Design life	8 yr
Waveband	5.4 GHz, 13.256 GHz
Spatial resolution	10 km, 20 km
Swath width	1400 km
Wind speed measurement range	3–50 m/s

Several studies have evaluated the accuracy and consistency of the FY-3 satellite's sensors [22], [23], [24], [25], [26]. For FY-3E WindRAD, Li et al. [27] aims to provide an overview of the characteristics of the Normalized Radar Cross Section (NRCS or σ°) obtained from the WindRAD Level-1 data. However, the accuracy of wind vectors derived from FY-3E WindRAD has not been evaluated extensively in terms of the spatial and temporal distribution of data errors over the global ocean during the mission period. The purpose of this study is to identify potential biases or errors in the FY-3E wind vectors. Specifically, we utilize reanalysis data and ground-truth buoy measurements to validate and analyze the accuracy and quality of wind field measurements provided by FY-3E WindRAD, with a particular focus on the spatiotemporal variations in wind field measurement errors. Through such analysis, our aim is to quantitatively assess FY-3E's wind field product, delineate the product's error characteristics, and provide valuable insights for optimizing and utilizing FY-3E wind field data. This is particularly significant for the research of the next-generation dual-band dual-polarization wind field inversion algorithms.

The remainder of the paper is structured as follows. Section II provides a brief overview of the FY-3E WindRAD instrument and its data retrieval algorithms, as well as describing the methodology used to evaluate the wind field data quality and accuracy. Section III presents the results of the study, including the identification of potential biases and error sources, and the evaluation of the impact of error distribution in both time and space. Finally, Section IV concludes the paper and discusses the implications of the findings for future research and applications.

II. MATERIALS AND METHODS

A. FY-3E WINDRAD WIND FIELD PRODUCT

For the FY-3E WindRAD wind field product, the C-band model 5.N (CMOD5.N) [28] was utilized for estimating wind speed. This estimation was achieved through maximum likelihood estimation (MLE), accomplished by comparing the observed σ_m^0 with the simulated σ_s^0 based on the background wind speed input [29], [30]. The MLE technique seeks to maximize the likelihood of obtaining the observed σ_m^0 given the background wind speed input and the model parameters [27]. Additionally, the multi-scale superposition (MSS) method [31] is employed to generate a set of solutions, which serve as the initial guess for the two-dimensional variational (2DVAR) method [32]. The 2DVAR method, utilizing the ECMWF High-Resolution Ensemble Forecast System (HRES) wind product as the background, is employed to obtain the final wind field inversion results.

$$MLE_C = \frac{1}{N}\sum_{i=1}^{N}\frac{(\sigma_{mi}^0 - \sigma_{si}^0)^2}{(K_p(\sigma_{mi}^0))^2}, \tag{1}$$

where, σ_{mi}^0 represents the measured backscatter coefficient, σ_{si}^0 is the simulated backscatter coefficient, K_p signifies the

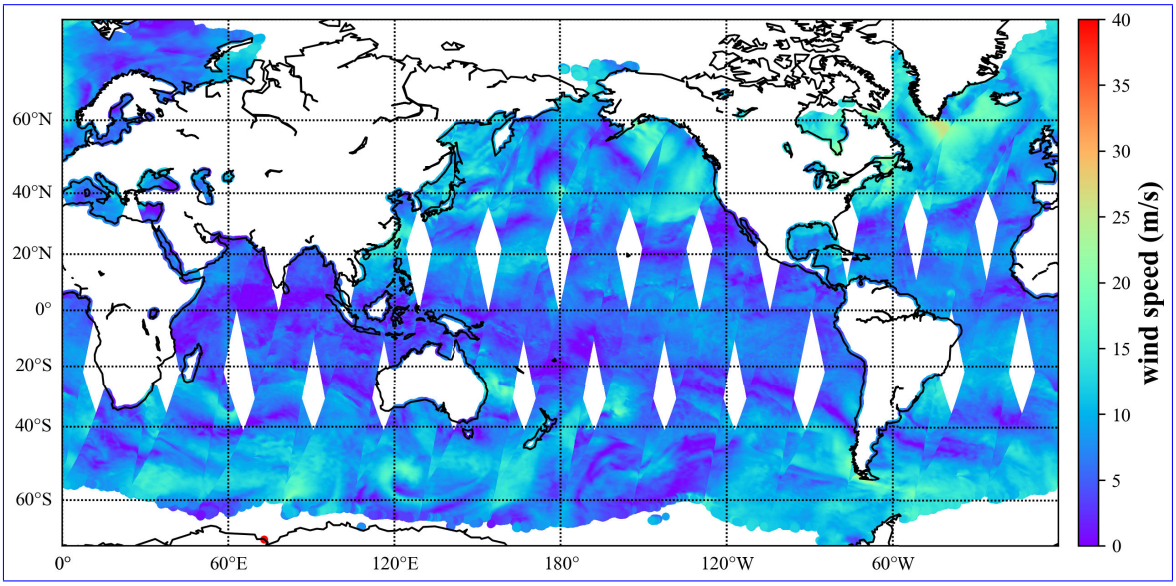

FIGURE 1. Global coverage of the FY-3E WindRad scatterometer for a single day (December 1, 2022).

expected Gaussian observation noise, and N corresponds to the number of views in the wind vector cell (WVC).

In this study, we selected the first batch of publicly available FY-3E WindRAD wind field products based solely on the C-band VV polarization data sourced from the FENGYUN Satellite Data Center (http://satellite.nsmc.org.cn /portalsite/default.aspx, accessed on March 1, 2023). These data encompass the time period from June to December 2022 and possess a spatial resolution of 10 km. To ensure the data's validity, we applied quality control measures to the observations. Specifically, we employed bits 7 to 16 of the 17-bit binary code for quality control (Table 2). In regions characterized by high latitudes, efforts were made to eliminate the influence of ice on the observations (Bit 14, "Some portion of WVC is over ice"). This study aims to investigate the spatiotemporal characteristics of the wind speed obtained from FY-3E remote sensing and the associated error. The duration of the data examined in this study is approximately 7 months, which limits its suitability for capturing climatological features. However, the novelty of our work stems from the detailed analysis of temporal and spatial variations in and wind direction retrievals during a specific period, namely June to December 2022.

Figure 1 depicts the global coverage of the FY-3E WindRad scatterometer for a 24-hour period on December 1, 2022. The scatterometer on the FY-3E satellite provides high-resolution ocean surface wind field measurements globally. As a result of its polar orbit with an inclination of 98.73°, the satellite covers the Earth's entire surface twice a day, and the scatterometer is thus able to measure the wind field over the oceans around the world twice within a 24-hour period.

B. ERA5 REANALYSIS PRODUCT

The FY-3E WindRad L2 level product data from June 1, 2022 to December 31, 2022 were matched with reanalysis data for verification. The fifth-generation reanalysis dataset (ERA5) is a global atmospheric reanalysis dataset produced by ECMWF (https://www.ecmwf.int/en/forecasts/dataset/ecmwf-reanalysis-v5, accessed on March 1, 2023). It provides comprehensive and high-quality information about the Earth's atmosphere, including various meteorological variables such as wind, temperature, precipitation, pressure, and more. It covers the period from 1979 to present and provides a consistent view of the atmospheric state at high temporal and spatial resolution. The used dataset has a 0.25° horizontal resolution and an hourly temporal resolution. It includes a range of meteorological parameters, such as temperature, wind speed, and precipitation, and provides extensive coverage of both the atmosphere and the surface.

To compare with the satellite observations, the neutral wind u and v components, as well as the grid longitude, latitude, and time information, were extracted from the FY-3E data. Subsequently, the ERA5 data were interpolated linearly in spatial to match the satellite observation pixels within a time window of 30 minutes. By comparing the satellite-derived wind data with the ERA5 reanalysis product from ECMWF,

TABLE 2. Description of Quality Flags for Wind Vector Retrieval. Quality flag is designed for the 17-bit (Bit0-16) binary code, and each 0 or 1 indicates good or bad quality.

Flag Bit	Description
7	Distance to GMF too large
8	No meteorological background used
9	Rain detected
10	Rain flag not usable
11	Wind speed less than or equal to 3 m/s
12	Wind speed greater than 30 m/s
13	Wind inversion not successful
14	Some portion of WVC is over ice
15	Some portion of WVC is over land
16	Not enough good σ_0 for wind retrieval

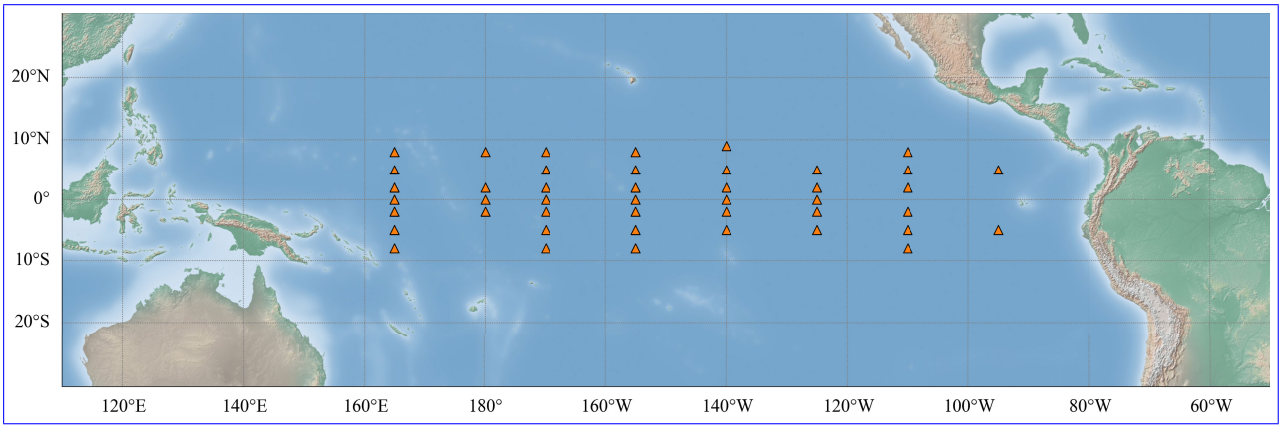

FIGURE 2. Array configuration of the Tropical Atmosphere/Ocean (TAO) in the tropical Pacific Ocean.

the study aims to evaluate the consistency and agreement, thereby providing insights into the reliability and utility of the satellite-based wind retrieval approach.

C. TAO/TRITON ARRAY

In order to assess the accuracy of the FY-3E WindRad L2 level winds product, we have incorporated valuable data from the Tropical Atmosphere/Ocean (TAO) array (https://tao.ndbc.noaa.gov/tao/data_download/search_map.shtml, accessed on October 1, 2023), which was renamed the TAO/TRITON (Triangle Trans-Ocean Buoy Network) array on January 1, 2000. This array comprises 61 strategically placed moorings situated across the Tropical Pacific Ocean, as depicted in Figure 2. These moorings play a pivotal role in continuously monitoring oceanographic and meteorological conditions in real-time and can serve as ground truth data for verifying and analyzing the accuracy of FY-3E's wind field measurements.

To ensure the utmost precision in our evaluation process, we have specifically focused on utilizing wind speed and wind direction data sourced from the TAO/TRITON array. Our criteria for data selection included a requirement for measurements to be within close proximity, specifically within a 25 km, and temporal alignment within a ±5-minute window. This meticulous spatiotemporal alignment of data is instrumental in enhancing the precision and relevance of our comparative analysis. The integration of data from the TAO/TRITON moored buoys into our evaluation framework not only bolsters the accuracy of our assessment but also ensures that our findings are robust and reliable.

D. METRICS

The results are compared with ERA5 and wind measurements from the TAO/TRITON array to understand the dynamic range and scale features of the FY-3E wind speed. The study also examines the error characteristics of differences between FY-3E and ERA5 wind speeds to understand the temporal and spatial variation patterns of FY-3E wind speed bias and accuracy. To compare the accuracy of remote sensing products, a commonly used metric is the standard deviation (STD), which quantifies the difference (bias) between retrievals and observed values. Another metric is the correlation coefficient R, which measures the degree of linear relationship between the retrievals and observed values. By comparing them with ERA5 and TAO/TRITON data, these three metrics are calculated to understand the performance and characteristics of FY-3E wind speed, providing valuable insights for enhancing the applications of FY-3E wind field data.

III. RESULTS

A. OVERALL PERFORMANCE

1) COMPARISON OF FY-3E AND ERA5

In order to systematically assess the accuracy of FY-3E wind speed and direction retrievals without quality control, we compared the data with ERA5. As shown in Figure 3a, the STD of FY-3E wind speed retrievals compared to ERA5 data is 1.44 m/s, indicating a strong agreement and highlighting the high stability of the FY-3E product. However, in regions with lower wind speeds, some discrepancies were observed, with FY-3E wind speed retrievals tending to be slightly higher than ERA5 data. Considering the actual variability of sea surface winds in low wind conditions, the wind speed measurement range for FY-3E was designed to cover 3 to 50 m/s. To ensure precise wind direction measurements, the evaluation was specifically focused on wind speeds exceeding 3 m/s. Following the exclusion of outliers identified by the quality flags detailed in Table 2, the FY-3E dataset is subsequently reduced. Nevertheless, the fundamental statistical metrics exhibit minimal alteration. Specifically, the STD remains at 1.45 m/s, the bias is maintained at −0.42 m/s, and the correlation coefficient stands at 0.91. From the distribution observed in Figure 3c, it is apparent that in regions with lower wind speeds, the anomalous wind speed retrievals of FY-3E have been filtered out, retaining high-quality data.

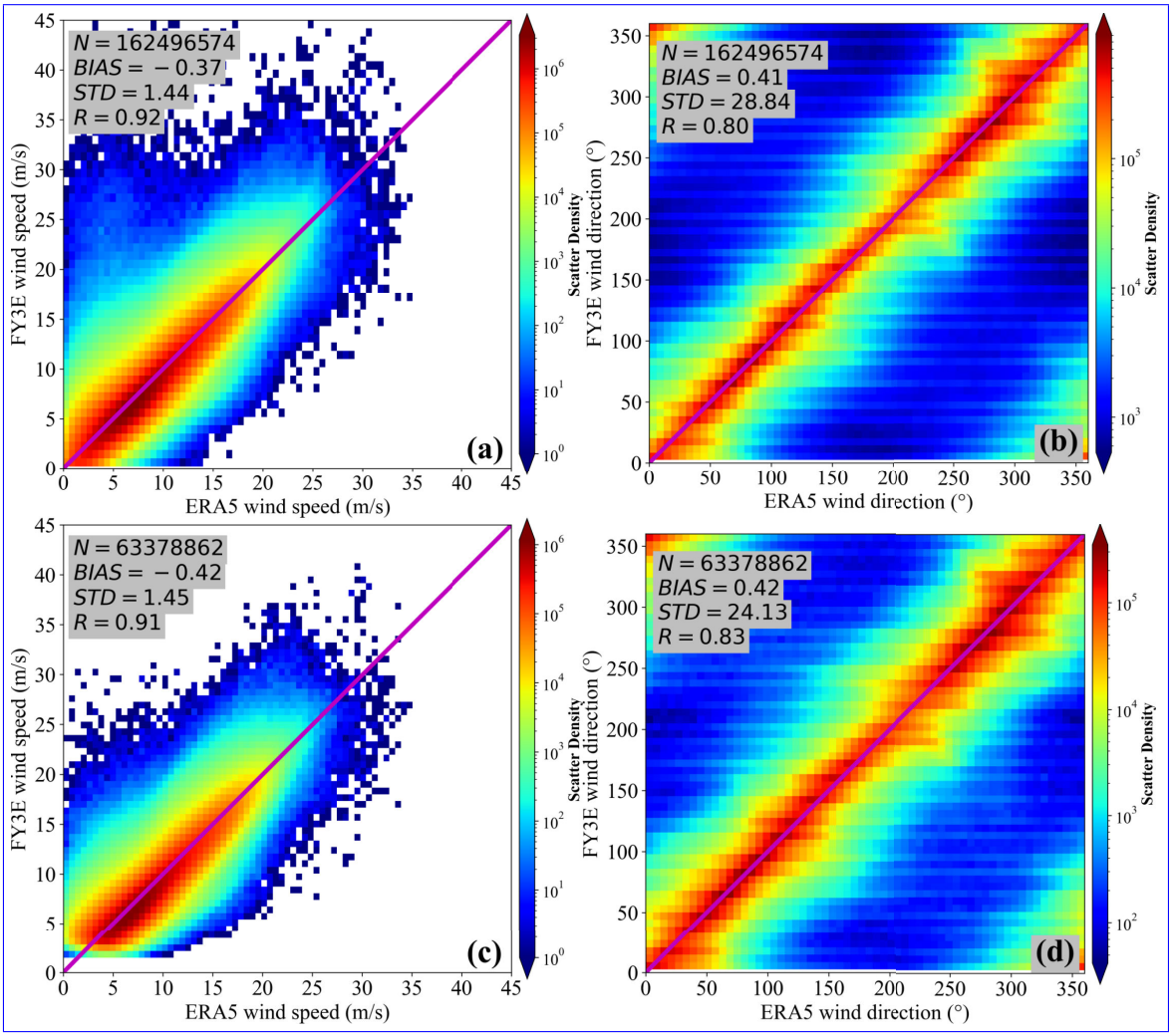

FIGURE 3. Comparison of FY-3E WindRad L2 product data accuracy before (a,b) and after (c,d) quality control using ECMWF ERA5. *N* is the number of matchups.

Furthermore, FY-3E wind direction retrievals were compared to ERA5 data. In Figure 3b, the unfiltered FY-3E retrievals exhibited a correlation coefficient (R) of 0.80 and a STD of 28.84° when compared to ERA5 data. In Figure 3 d, we present the scatter plot after applying quality control, which shows an improved data distribution with outliers removed, resulting in enhanced data accuracy. Specifically, the STD between FY-3E and ERA5 was reduced to 24.13°, and the correlation coefficient (R) increased to 0.83. These findings indicate that after quality control, FY-3E wind speed and direction retrievals agree well with ERA5 data.

In order to analyze the accuracy of FY-3E wind speed retrievals across different wind speed ranges with respective to ERA5 winds, a range-dependent analysis was conducted. This analysis examined the differences between FY-3E wind speed retrievals and ERA5 wind speeds within different wind speed intervals, with the goal of identifying any biases or trends in the accuracy of wind speed retrievals across different wind speed ranges. A bin-wise analysis of FY-3E wind speed retrievals in 2 m/s intervals within the range of 0-20 m/s was conducted as shown in Figure 4a. The moderate wind speed (2-10 m/s) has a large amount of wind speed data as shown in Figure 3a, and the deviation in the evaluation of FY-3E wind speed inversion is relatively small, which can obtain a more accurate evaluation of product performance. The distribution of biases reveals two distinct characteristics: those smaller than 2 m/s (approximately 2.5 m/s) and those larger than 3 m/s (approximately −0.4 m/s), which are entirely opposite in nature. This phenomenon can be attributed to the design of FY-3E 's WindRad sensor, which is designed to operate within the range of 3 to 50 m/s.

To analyze the accuracy of FY-3E wind direction retrievals, a similar approach was taken as for wind speed. A bin-wise analysis of FY-3E wind direction retrievals in 60° intervals within the range of 0°–360° was conducted to examine the differences between FY-3E wind direction retrievals and reanalysis data, with the goal of identifying any biases or trends in the accuracy of wind direction retrievals across different wind direction ranges, as shown in Figure 4 b. The results showed that the FY-3E wind direction retrievals

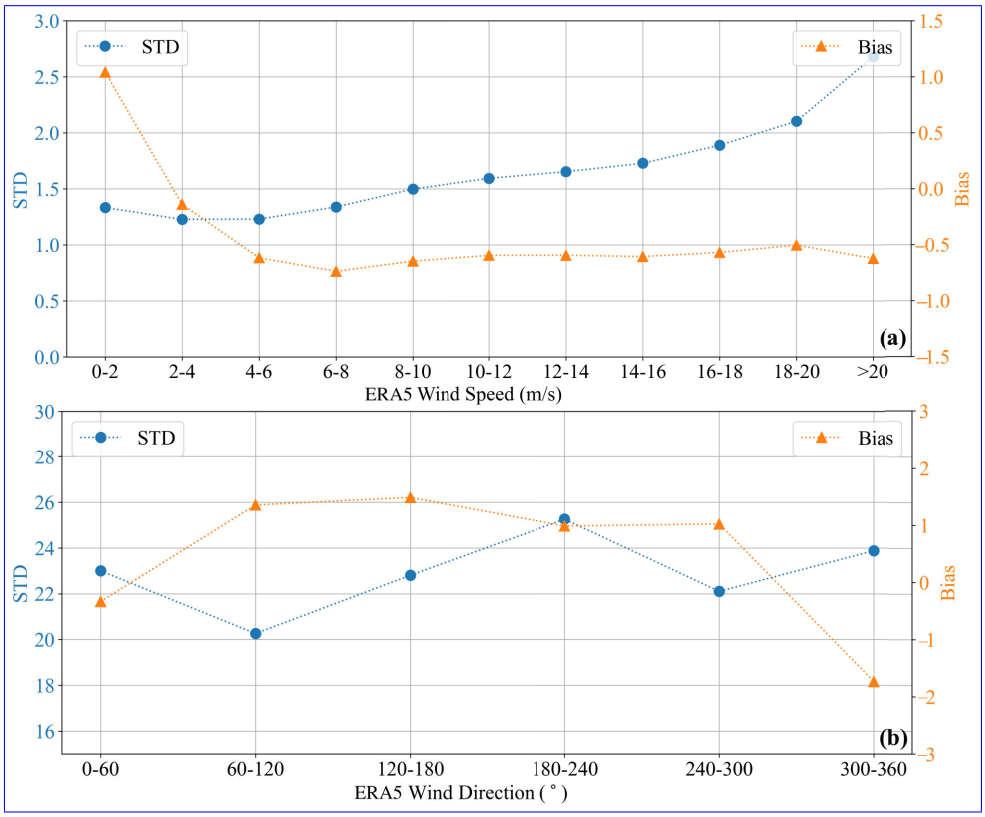

FIGURE 4. Accuracy assessment of FY-3E WindRad L2 Level product compared with ERA5 in various (a) wind speed and (b) wind direction intervals.

have an STD of approximately 23 ° in most wind direction intervals, as shown in Figure 4. The singularity in the retrieval algorithm is caused by the inverse tangent function that is used to calculate wind direction from the east–west and north–south components of the wind. As the wind direction approaches 0° or 360°, this function becomes highly sensitive to small changes in the input data, leading to increased uncertainties and errors in the retrieved wind direction. This is a well-known challenge in satellite-based wind retrievals and is often mitigated through the use of more sophisticated retrieval algorithms or additional measurements to improve the accuracy of the retrievals.

2) COMPARISON OF FY-3E AND TAO/TRITON

To comprehensively evaluate the FY-3E WindRad L2 Level product, we have enhanced the persuasiveness of our assessment. In addition to the comparison with ERA5 data, this study also utilizes ground-truth measurements from the TAO/TRITON array to evaluate the accuracy of the FY-3E WindRad product. This additional dimension of evaluation further strengthens the credibility of our research findings.

By comparing FY-3E WindRad product's wind speed and wind direction retrievals with the invaluable dataset from the TAO/TRITON array, our analysis has unveiled remarkable results. The reported wind speed accuracy, as quantified by the STD, impressively stands at 1.37 m/s (Figure 5a). Additionally, the wind direction STD is registered at 36.41° (Figure 5b). This also serves as empirical evidence confirming the consistency of the FY-3E WindRad L2 product, aligning not only with state-of-the-art ERA5 data but also showing comparability with ground-truth measurements obtained from the TAO/TRITON array.

B. TEMPORAL CHARACTERISTICS

To analyze the distribution of time-dependent bias and STD in the FY-3E sea surface wind product, the temporal characteristics of FY-3E remote sensing wind speed were investigated by analyzing the variability of wind speed. The differences between FY-3E wind speed retrievals and ERA5 wind speeds over the period of June to December in 2022 were examined, with a focus on identifying any trends or patterns in the temporal distribution of wind speed bias and STD.

Figure 6 demonstrates the temporal analysis results, which indicate temporal variations in the distribution of wind speed bias. In November 2022, three optimizations were applied to FY-3E wind field retrievals, involving improved data quality control, updated MSS method with 144 solutions spaced at 2.5°, and real-time ocean calibration bias correction [27]. Specifically, the strict quality control scheme ensures the selection of high-quality data, which helps to reduce measurement errors and minimize the influence of environmental factors such as the incidence angle. The updated MSS removal method effectively removes the ambiguous

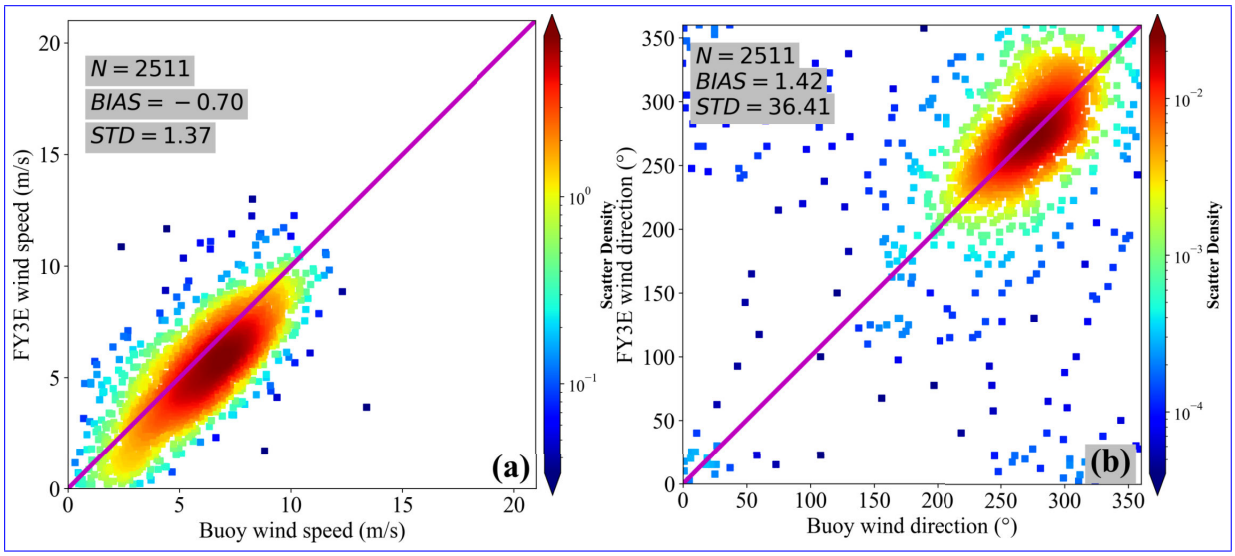

FIGURE 5. Scatterplot depicting the FY-3E WindRad L2 Level product in relation to TAO/TRITON observations, specifically illustrating (a) wind speed and (b) wind direction.

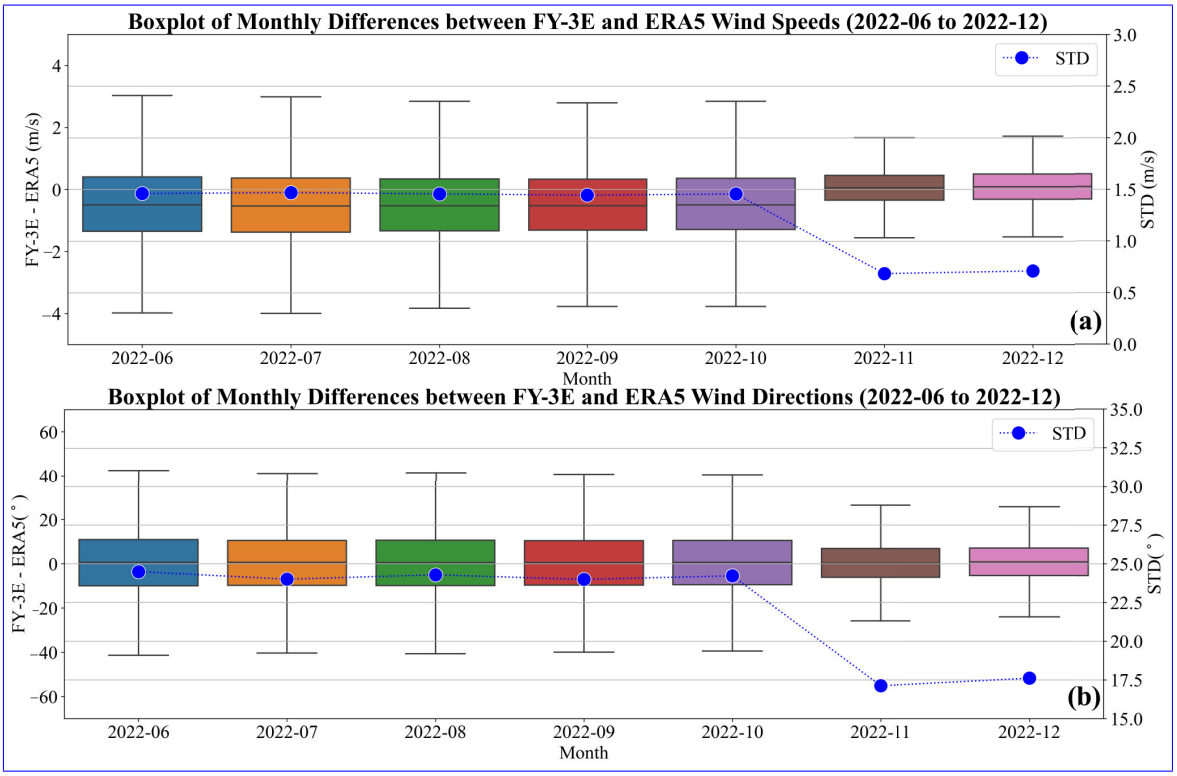

FIGURE 6. Temporal characteristics of FY-3E WindRad L2 Level Product (Optimizations of the FY-3E wind field retrieval algorithm were implemented in November 2022). The boxes depicted in the plots represent the interquartile range (IQR), which encompasses the middle 50% of the data. Within the box, the line represents the median, while the whiskers extend to the most extreme data points located within 1.5 times the IQR from the edges of the box.

solutions caused by multiple scattering effects, which in turn improves the accuracy of wind speed and direction retrieval. Moreover, the implementation of the ocean calibration bias correction significantly reduces the influence of systematic errors in wind field retrieval, particularly over ocean regions, resulting in a more accurate and consistent wind field product.

As well as the distribution of wind speed deviation over time, the influence of time-dependent errors on the accuracy of FY-3E wind speed retrievals was also explored.

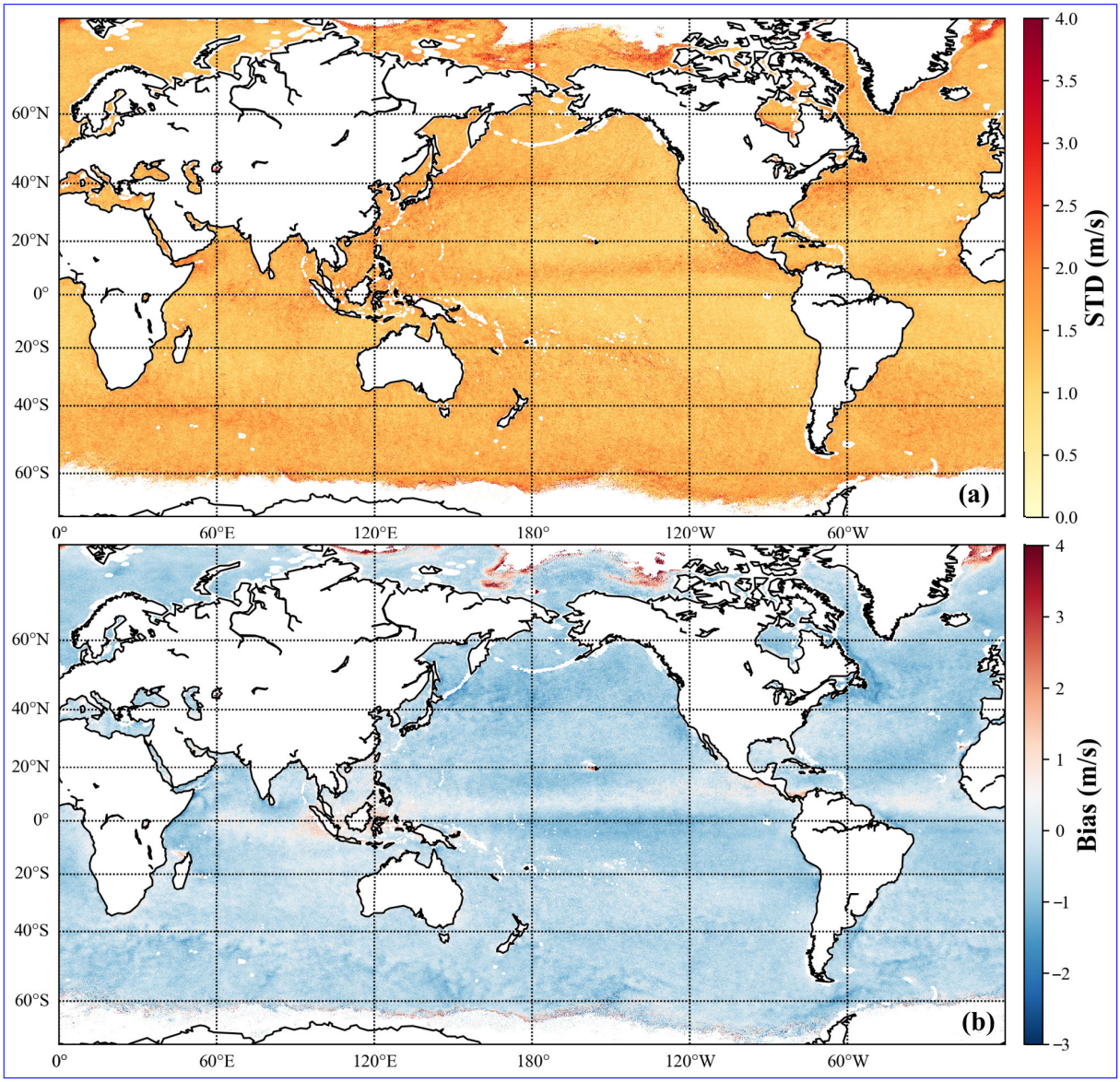

FIGURE 7. Global 0.1° gridded map of the bias and STD of FY-3E WindRAD wind speed computed against ERA5 over the period of June to December in 2022.

By analyzing the bias and standard deviation for each month, it was observed that the performance of the FY-3E product remained consistent both before and after November 2022 as shown in Figure 6. We observed that the bias of FY-3E was slightly higher in November and December but has now moved closer to zero. The shorter boxes in Figure 6 indicate a more concentrated data distribution, and the shorter error bars represent lower STD. From a relative perspective, the performance of FY-3E in November 2022 and December 2022 is now shown to be closer to ERA5 data. This indicates that the accuracy of FY-3E wind speed retrievals is relatively unaffected by time-dependent errors, highlighting the robustness of the method in accounting for temporal variations in FY-3E remote sensing wind speed data.

Wind direction retrieval is particularly challenging, owing to the complex nature of the underlying physical processes that govern wind direction. An evaluation of FY-3E wind direction accuracy reveals that the bias is relatively stable over the period of June to December in 2022 (Figure 6). The stability of the bias in FY-3E wind direction is an encouraging finding, since it indicates that the instrument has a consistent systematic error. Two distinct periods, namely June to October and November to December, demonstrate relatively stable characteristics in terms of wind direction STD. Based on the analysis of the temporal distribution of FY-3E's wind direction STD, the study demonstrates a significant improvement in STD following the recent updates implemented for FY-3E.

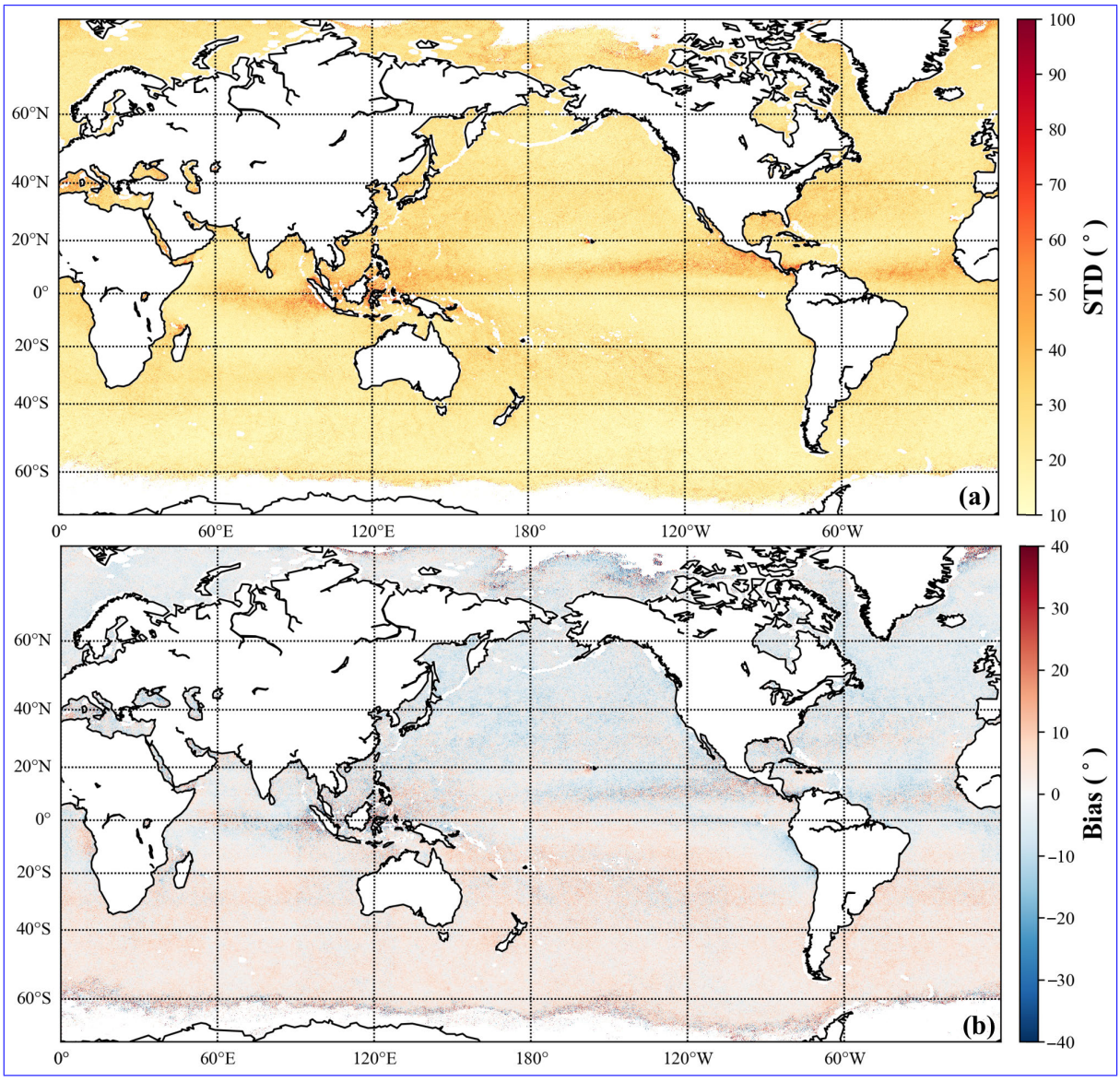

FIGURE 8. Global 0.1° gridded map of the bias and STD of the FY-3E WindRAD wind direction computed against ERA5 over the period of June to December in 2022.

C. SPATIAL CHARACTERISTICS

To systematically evaluate the spatial distribution of FY-3E wind speed errors, we selected along-track data and used the ERA5 data as a reference for visualization and analysis. The wind product itself has a resolution of approximately 10 km × 10 km, meaning that each grid cell represents an area of 10 km×10 km on the Earth's surface. This resolution provides a detailed depiction of the wind patterns and allows for the identification of localized variations in wind speed and direction. Analysis of the spatial distribution of the FY-3E remote sensing wind speed bias reveals that the bias is generally small over oceanic regions, as shown in Figure 7. By utilizing a 0.1 degree gridded map, the figures effectively showcase the spatial distribution and variations in the wind field captured by the FY-3E WindRad instrument.

Based on the spatial distribution of the FY-3E wind speed bias, it is evident that negative biases are prominent across various regions. In addition, there are visible positive and negative bias stripes along the equator, especially in the Pacific region. However, some spatial discrepancies can be found between FY-3E and ERA5 wind speeds in certain regions. The presence of sea ice can significantly affect the accuracy of wind retrievals near ice shelves, as the radar return from sea ice is much stronger than from open water, resulting in erroneous high-speed wind estimates. Moreover, the ERA5 wind speed biases could potentially impact various fields that rely on accurate wind speed measurements from FY-3E. There are indeed significant spatial variations in the STD of the FY-3E wind speed, as depicted in Figure 7. These variations indicate that the errors in FY-3E are not

uniform across different regions and can differ in magnitude depending on their locations. This may indicate that the errors in FY-3E retrievals are primarily time-dependent rather than spatially dependent. Further research is needed to determine the primary sources of errors in FY-3E retrievals and their spatial and temporal characteristics.

In contrast to the wind speed, the FY-3E wind direction exhibits strong similarity in the spatial distributions of its bias and STD, as shown in Figure 8. In regions where the FY-3E wind direction bias is large, its STD is also large. These regions are mainly located near the equator in the eastern Pacific, along the western coast of South America, and in the coastal waters on both sides of Africa. These spatial distribution characteristics of the FY-3E wind speed can provide valuable insights into the performance of the FY-3E remote sensing wind speed measurements.

IV. CONCLUSION AND DISCUSSION

The novelty of this study lies in the detailed analysis of FY-3E WindRAD wind speed data during a specific period, encompassing spatiotemporal variations and wind direction retrievals in comparison to both ERA5 data and real-time TAO/TRITON measurements. This analysis provides a deeper understanding of the characteristics and performance of the wind dataset. The comparative analysis between FY-3E and ERA5 from June 1, 2022, to December 31, 2022, revealed that FY-3E wind speed retrievals exhibited an overall bias of −0.42 m/s and a STD of 1.45 m/s. Furthermore, when compared to ground-truth observations obtained from the TAO/TRITON array, our analysis indicated a bias of −0.70 m/s and an STD of 1.37 m/s for wind speed retrievals.

The analysis has unveiled notable temporal variations in the bias and STD, providing strong evidence of a significant enhancement in FY-3E's performance due to the recent updates. However, it's worth noting that time-dependent errors have a less pronounced impact on the accuracy of FY-3E wind speed retrievals. When examining the spatial distribution of bias and STD, we observed that certain regions exhibited relatively high values, which are likely influenced by the complex nature of ice contamination in those areas. Our research findings regarding the accuracy and characteristics of FY-3E WindRAD provide valuable insights for optimizing and leveraging FY-3E wind field product. This research holds particular significance in advancing the development of next-generation dual-band dual-polarization wind field inversion algorithms.

ACKNOWLEDGMENT

The authors acknowledge the support of the FengYun Satellite Data Center in providing the data, status, and mission information. They would like to acknowledge the use of ECMWF ERA5 winds in their research. These data were essential in providing accurate and reliable wind information for our study. They greatly appreciate the efforts of ECMWF in producing and providing these high-quality data products. They extend their heartfelt gratitude to the TAO/TRITON buoy data. These invaluable observational data have provided an indispensable foundation for their research, enabling them to delve deeply into the evaluation of the FY-3E WindRad product's performance.

REFERENCES

[1] S. Alsweiss, R. Hanna, P. Laupattarakasem, W. Jones, C. Hennon, and R. Chen, "A non-MLE approach for satellite scatterometer wind vector retrievals in tropical cyclones," *Remote Sens.*, vol. 6, no. 5, pp. 4133–4148, May 2014, doi: 10.3390/rs6054133.

[2] Z. Wang and C. Zhao, "Assessment of wind products obtained from multiple microwave scatterometers over the China Seas," *Chin. J. Oceanol. Limnol.*, vol. 33, no. 5, pp. 1210–1218, Sep. 2015, doi: 10.1007/s00343-015-4124-8.

[3] E. P. W. Attema, "The active microwave instrument on-board the ERS-1 satellite," *Proc. IEEE*, vol. 79, no. 6, pp. 791–799, Jun. 1991, doi: 10.1109/5.90158.

[4] F. J. Wentz, D. K. Smith, C. A. Mears, and C. L. Gentemann, "Advanced algorithms for QuikScat and SeaWinds/AMSR," in *Proc. IEEE Int. Geosci. Remote Sens. Symp.*, Jul. 2001, pp. 1079–1081, doi: 10.1109/IGARSS.2001.976752.

[5] J. Figa-Saldaña, J. J. W. Wilson, E. Attema, R. Gelsthorpe, M. R. Drinkwater, and A. Stoffelen, "The advanced scatterometer (ASCAT) on the meteorological operational (MetOp) platform: A follow on for European wind scatterometers," *Can. J. Remote Sens.*, vol. 28, no. 3, pp. 404–412, Jan. 2002, doi: 10.5589/m02-035.

[6] M. A. Bourassa, M. H. Freilich, D. M. Legler, W. T. Liu, and J. J. O'Brien, "Wind observations from new satellite and research vessels agree," *Eos, Trans. Amer. Geophys. Union*, vol. 78, no. 51, pp. 597–602, Dec. 1997, doi: 10.1029/97eo00357.

[7] X. Dong, D. Zhu, J. Zhu, and T. Wang, "Progresses of development of CFOSAT scatterometer," in *Proc. IEEE Int. Geosci. Remote Sens. Symp.*, Jul. 2012, pp. 237–240, doi: 10.1109/IGARSS.2012.6351594.

[8] D. Hauser, C. Tison, T. Amiot, L. Delaye, A. Mouche, G. Guitton, L. Aouf, and P. Castillan, "CFOSAT: A new Chinese–French satellite for joint observations of ocean wind vector and directional spectra of ocean waves," *Proc. SPIE*, vol. 9878, May 2016, Art. no. 98780T, doi: 10.1117/12.2225619.

[9] X. Jiang, M. Lin, J. Liu, Y. Zhang, X. Xie, H. Peng, and W. Zhou, "The HY-2 satellite and its preliminary assessment," *Int. J. Digit. Earth*, vol. 5, no. 3, pp. 266–281, May 2012.

[10] Z. Li, A. Stoffelen, and A. Verhoef, "A generalized simulation capability for rotating-beam scatterometers," *Atmos. Meas. Techn.*, vol. 12, no. 7, pp. 3573–3594, Jul. 2019.

[11] D. Hauser et al., "New observations from the SWIM radar on-board CFOSAT: Instrument validation and ocean wave measurement assessment," *IEEE Trans. Geosci. Remote Sens.*, vol. 59, no. 1, pp. 5–26, Jan. 2021.

[12] K. Zhao, C. Zhao, and G. Chen, "Evaluation of Chinese scatterometer ocean surface wind data: Preliminary analysis," *Earth Space Sci.*, vol. 8, no. 7, Jul. 2021, Art. no. e2020EA001482, doi: 10.1029/2020EA001482.

[13] H. Ye, J. Li, B. Li, J. Liu, D. Tang, W. Chen, H. Yang, F. Zhou, R. Zhang, S. Wang, and S. Tang, "Evaluation of CFOSAT scatterometer wind data in global oceans," *Remote Sens.*, vol. 13, no. 10, p. 1926, May 2021, doi: 10.3390/rs13101926.

[14] M. Lin and Y. Zhang, "Current status and main application achievements of ocean satellites," *Chin. J. Space Sci.*, vol. 42, no. 4, pp. 733–743, 2022, doi: 10.11728/cjss2022.04.yg4.

[15] P. Chakraborty, R. Jyoti, and P. Gupta, "An advanced Ku-band fine-resolution and high-sensitivity wind scatterometer," *IEEE Trans. Geosci. Remote Sens.*, vol. 61, 2023, Art. no. 5104507.

[16] R. Tardif and S. Laroche, "An equivalent neutral wind observation operator for variational assimilation of scatterometer ocean surface wind data," *Quart. J. Roy. Meteorol. Soc.*, vol. 138, no. 669, pp. 2086–2104, Oct. 2012, doi: 10.1002/qj.2569.

[17] F. Mao, Q. Min, G. Liu, C. Liu, S. Feng, S. Jin, J. Hu, W. Gong, and C. Li, "Assimilating moderate resolution imaging spectroradiometer radiance with the weather research and forecasting data assimilation system," *J. Appl. Remote Sens.*, vol. 11, no. 3, Jul. 2017, Art. no. 036002, doi: 10.1117/1.jrs.11.036002.

[18] I. Gultepe et al., "A review of high impact weather for aviation meteorology," *Pure Appl. Geophys.*, vol. 176, no. 5, pp. 1869–1921, May 2019, doi: 10.1007/s00024-019-02168-6.
[19] P. Zhang, X. Hu, Q. Lu, A. Zhu, M. Lin, L. Sun, L. Chen, and N. Xu, "FY-3E: The first operational meteorological satellite mission in an early morning orbit," *Adv. Atmos. Sci.*, vol. 39, no. 1, pp. 1–8, Jan. 2022, doi: 10.1007/s00376-021-1304-7.
[20] X. Shi, B. Duan, and K. Ren, "F2F-NN: A field-to-field wind speed retrieval method of microwave radiometer data based on deep learning," *Remote Sens.*, vol. 14, no. 15, p. 3517, Jul. 2022. [Online]. Available: https://www.mdpi.com/2072-4292/14/15/3517
[21] H. Yin, Z. Fan, and F. Dou, "System characteristics design of WindRadar on FengYun-3E meteorological satellite," *Proc. SPIE*, vol. 9264, Nov. 2014, Art. no. 92641I, doi: 10.1117/12.2068933.
[22] H. Wang, L. Guan, and G. Chen, "Evaluation of sea surface temperature from FY-3C VIRR data in the Arctic," *IEEE Geosci. Remote Sens. Lett.*, vol. 13, no. 2, pp. 292–296, Feb. 2016, doi: 10.1109/LGRS.2015.2511184.
[23] Z. Liao, Q. Dong, and C. Xue, "Evaluation of sea surface temperature from FY-3C data," *Int. J. Remote Sens.*, vol. 38, no. 17, pp. 4954–4973, Sep. 2017, doi: 10.1080/01431161.2017.1331058.
[24] Q. He, Y. Zhang, and J. Wang, "Development and evaluation of regional SST regression algorithms for FY-3C/VIRR data in the Western North Pacific," *Remote Sens. Lett.*, vol. 11, no. 12, pp. 1090–1099, Dec. 2020, doi: 10.1080/2150704x.2020.1823034.
[25] Y. Sun, X. Wang, Q. Du, W. Bai, J. Xia, Y. Cai, D. Wang, C. Wu, X. Meng, Y. Tian, Y. Tian, C. Liu, W. Li, D. Zhao, F. Li, and H. Qiao, "The status and progress of Fengyun-3E GNOS II mission for GNSS remote sensing," in *Proc. IEEE Int. Geosci. Remote Sens. Symp. (IGARSS)*, Jul. 2019, pp. 5181–5184, doi: 10.1109/igarss.2019.8899319.
[26] F. Huang, J. Xia, C. Yin, W. Bai, Y. Sun, L. Duan, G. Yang, X. Hu, X. Xiao, X. Zhai, F. Yan, Q. Du, X. Wang, and Y. Cai, "Preliminary validation of FENGYUN-3E GNOS-II GNSS-R wind prodcut," in *Proc. IEEE Specialist Meeting Reflectometry GNSS Signals Opportunity (GNSS+R)*, Sep. 2021, pp. 61–64, doi: 10.1109/GNSSR53802.2021.9617683.
[27] Z. Li, A. Verhoef, A. Stoffelen, J. Shang, and F. Dou, "First results from the WindRAD scatterometer on board FY-3E: Data analysis, calibration and wind retrieval evaluation," *Remote Sens.*, vol. 15, no. 8, p. 2087, Apr. 2023, doi: 10.3390/rs15082087. [Online]. Available: https://www.mdpi.com/2072-4292/15/8/2087
[28] F. J. Wentz and D. K. Smith, "A model function for the ocean-normalized radar cross section at 14 GHz derived from NSCAT observations," *J. Geophys. Res., Oceans*, vol. 104, no. C5, pp. 11499–11514, May 1999, doi: 10.1029/98jc02148.
[29] C.-Y. Chi and F. K. Li, "A comparative study of several wind estimation algorithms for spaceborne scatterometers," *IEEE Trans. Geosci. Remote Sens.*, vol. GRS-26, no. 2, pp. 115–121, Mar. 1988, doi: 10.1109/36.3011.
[30] A. Stoffelen and M. Portabella, "On Bayesian scatterometer wind inversion," *IEEE Trans. Geosci. Remote Sens.*, vol. 44, no. 6, pp. 1523–1533, Jun. 2006, doi: 10.1109/TGRS.2005.862502.
[31] M. Arnús, "Wind field retrieval from satellite radar systems," Ph.D. dissertation, Dept. Astronom. Meteorol., Univ. Barcelona, Barcelona, Spain, Sep. 2002.
[32] J. Vogelzang, A. Stoffelen, A. Verhoef, J. de Vries, and H. Bonekamp, "Validation of two-dimensional variational ambiguity removal on SeaWinds scatterometer data," *J. Atmos. Ocean. Technol.*, vol. 26, no. 7, pp. 1229–1245, Jul. 2009, doi: 10.1175/2008jtecha1232.1.

YUE HE received the M.S. degree in remote sensing from Jilin University, Changchun, China, in 2007. She is currently with the Zhejiang Climate Center, Hangzhou, China. Her research interests include vegetation ecological monitoring and marine ecological element retrieval integrated satellite remote sensing and site monitoring data.

HE FANG received the Ph.D. degree in ocean remote sensing from the Nanjing University of Information Science and Technology, Nanjing, China, in 2019. He is currently with the Zhejiang Climate Center, Hangzhou, China. His research interest includes ocean wind measured by microwave radar remote sensing, especially hurricanes/typhoons imaged by synthetic aperture radar (SAR) over the ocean surface.

XIAOHUI LI received the M.S. degree in physical oceanography from the Second Institute of Oceanography, Ministry of Natural Resources, Hangzhou, China, in 2017, and the Ph.D. degree in communication and information system from Beihang University, Beijing, China, in 2021. He is currently with the Second Institute of Oceanography, Ministry of Natural Resources. He specializes in the field of ocean microwave remote sensing, storm surge numerical forecasting, and machine learning and its applications.

GAOFENG FAN received the B.S. degree in climate science from Nanjing University, Nanjing, China, in 1997, and the M.S. degree in software engineering from the Dalian University of Technology, Dalian, China, in 2008. He is currently with the Zhejiang Climate Center, Hangzhou, China. He has been engaged in research work in climate monitoring and diagnosis, extreme climate events and meteorological disaster assessment, risk zoning, and climate change assessment.

ZHONGHUA HE received the Ph.D. degree from the Institute of Remote Sensing and Digital Earth, Chinese Academy of Sciences, Beijing, China, in 2019. He is currently with the Zhejiang Climate Center, Hangzhou, China. His research interests include global carbon cycle research of biosphere-atmosphere interaction with multiple sources of satellite observation and data mining.

JUZHEN CAI received the B.S. degree in atmospheric physics from Nanjing University, Nanjing, China, in 1986. She is currently with the Zhejiang Climate Center, Hangzhou, China. Her research interests include climate feasibility application demonstration of megaproject and offshore wind energy assessment.